Vol. 45, No. 3 (2023) 375-386, DOI: 10.24874/ti.1426.12.22.06

Tribology in Industry

www.tribology.rs

RESEARCH

Influence of Nano-Lubrication On Tribological Behavior of AZ91 Magnesium Alloy Under Fretting Condition

Bharat Kumar[a], Shahid Saleem[a], M. F. Wani[a,*], Rakesh Sehgal[a], Sanjay Kumar[a]

[a]*Tribology Laboratory, Mechanical Engineering Department, National Institute of Technology Srinagar, Hazratbal, Srinagar, Kashmir- 190006, J&K (India)*.

Keywords:

Fretting
Friction
Wear
Magnesium alloy
Nano-lubrication
Lubricated fretting
Boundary lubrication

* Corresponding author:

M. F. Wani
E-mail: mfwani@nitsri.ac.in

Received: 22 December 2022
Revised: 28 January 2023
Accepted: 8 June 2023

A B S T R A C T

Fretting wear is very common damage found in parts under small-amplitude motion or vibration. Nano-lubrication is a very efficient way to reduce the friction and wear of mating parts. Therefore, fretting study was conducted on magnesium alloy (AZ91) under lubricating conditions using poly alpha olefin grade 4 (PAO4) with Graphite nanoparticles (NPs) (GNP) and hexagonal boron nitride (h-BN) NPs as lubricant additives. The experimental results reveal that the coefficient of friction (COF) and wear volume were reduced by 76% and 28%, respectively, using GNP and by 28% and 20%, respectively, using h-BN NPs. At optimal concentration of NPs, the effect of load on COF and wear was also investigated in this study. Wear volume and COF increases with increasing load. The performance of GNP was observed to be better as compared to h-BN NPs, which suggests its use as a lubricant additive in PAO4 as lubricated fretting conditions for AZ91 alloy. However, h-BN NPs perform well under higher loads.

1. INTRODUCTION

To enhance the performance of a system there is always a need to modify the system. The modifications can be in terms of design, working principle, process, and material of components. Material of component is a key parameter for deciding the performance of a system. Instanced research is going on for the advancement of materials in various fields. Researchers explored many advanced materials such as: lightweight materials [1], smart or intelligent materials [2], biomaterials [3,4], nano materials [5], corrosion resistant materials [6] etc. For structural purposes, the material should full fill the requirements of strength to withstand the load and optimized weight of the component. Magnesium alloys are low in density, have high specific strength, are well castable, machinable, weldable, and have strong corrosion resistance. These properties make magnesium alloys useful materials in automobiles and aircraft applications. Mordike and Ebert [7] and Mehta et al. [8] reported the magnesium alloy properties and their potential applications in various industries, particularly in the automobile industry. Several applications include the steering

wheel, dashboard mounting bracket, gearbox housing, transfer case and chassis components etc. In vehicles and aircrafts, various structural parts are made up of magnesium alloys such as AZ91 [9]. These components undergo vibrations during operation, which are transmitted to the structural parts and can cause micromotion between the parts in contact with each other.

Fretting is surface damage resulting from the plastic deformation of softer surfaces caused by low amplitude cyclic oscillating motion. [9,10]. Khabale and Wani [9] studied the fretting wear properties of AE41 and AZ91 under dry condition against AISI 52100 steel. Constant average COF with running time, marginal increment in COF with amplitude, and decrement in COF with applied normal load and oxidation, oscillation frequency was recorded. Adhesion, abrasion, and delamination were the principal wear mechanisms. AZ91 proved to have better wear resistance as compared to AE41.

Liang et al. [11] reported different wear regimes of AZ91 alloy. Under the steady-state condition, mild wear advances. The rate of wear under the severe wear regime constantly increases with the sliding distance. Delamination and oxidation were reported in mild wear regime, and plastic deformation and melting were reported in severe wear regime. Huang et al. [12] reported increasing wear with increasing load.

Researchers have put great efforts into the advancement of materials to enhance the tribological behavior of the system. One of the most efficient methods to improve the tribological behavior of the system is lubrication. Various additives are used to increase the tribological properties of lubricants [13,14]. Nano-lubrication is considered one of the most appropriate methods of improving the tribology of materials under various operating conditions [15]–[20]. Carbon nano additives are very promising in reducing the friction and wear of a tribological system. Many researchers studied the application of carbon nano additives in lubricants in the form of nanoparticles, nanotubes, nanosheets etc. and reported the enhancement of the tribological properties of the lubricants [15,17,21]. Lee et al. [15] reported that the COF on the coated plate was lower when comparing the GNP-coated plate to the base lubricant. Saini et al. [22] investigated the extreme pressure (EP) and anti-wear performance of Talc nanoparticles (NPs) in various lubricants. Zheng et al. [16] reported a reduction in COF by 70.2 % and in wear volume by 65.8 % using PAO4 dispersed with WS_2 for graphene nanocomposites. Reduction of COF by 0.057 and wear coefficient by 60-70% was reported by Kumar and Wani [17] when using Graphene oxide NPs in SAE20W50 lubricant. Charoo and Wani [18] reported a reduction in wear by 30 to 70 % by using h-BN NPs in SAE 20W50. The COF reduces by more than 40 % by using diamond NPs (0.5 weight %), and the wear scar diameter of nano-Si_3N_4/nano-SiC reduces by 140 μm using the diamond NPs mixed with mineral oil [18]. A friction reduction of 35.89 % and wear volume reduction of 20.86 % was reported by Srivyas and Charoo [23] by adding graphene nano-platelets in PAO4 lubricant. Tribological properties of Al-Si alloy against chrome plated steel balls improve under nano-lubrication using PAO4 mixed with h-BN NPs as EP additives [24].

PAO is made up of oligomers of hydrogenated olefins, with the general formula C_nH_{2n+2}. These high-performance base oils for motor oils, hydraulic fluids, transmission fluids, etc. developed using synthetic hydrocarbons [25]. They also have a higher viscosity index than mineral oils. Syed and Wani [26] and Fayaz and Wani [27] studied the compression of tribological behavior of the SAE9254 ring under lubrication starvation, boundary lubrication and mild EP lubrication conditions. The tribological tests were performed on a chromium coated SAE9254 grade steel piston ring against R185220 grade grey cast iron cylinder liner. Triaryl phosphate was added to PAO10 as EP additive to form EP-PAO10 (extreme pressure lubricant). EP-PAO10 reduces the COF by 74.1 % when compared to dry sliding conditions. GNP forms a protective film at the interface during sliding, which reduces friction and wear. Results show that nano-lubrication reduces friction and wear drastically at high-temperature sliding [28].

The development in the lubricants is taking place at a faster pace. Zinc dialkyldithiophosphate (ZDDP) proved to be an exceptional anti-wear additive in engine oil by forming tribofilm [29]. The use of ZDDP also cause electrolytic corrosion due to the presence of zinc [30]. The presence of sulphur, phosphorous and zinc causes ash formation which can results in reducing the effectiveness of catalyst in exhaust system and can block the filters [31]. So, finding a better alternative is essential for engine tribology.

As AZ91 is a promising material for high strength with light weight requirement of the components. Some of these components undergo vibrations which can result in wear of the components at the contacts. Very few researchers studied the fretting wear of this material. The fretting study of AZ91 under lubrication condition has not been performed previously. This work aims to investigate the tribological behavior of AZ91 under lubricated fretting condition. Tribological experiments were conducted on a ball (AISI-52100 steel) on disk (AZ91) tribo-pair using PAO4 with 0.1 weight % GNP and 0.1 weight % h-BN NPs under fretting condition. To determine the properties of prepared nanolubricants, the rheological tests were also conducted on a modular compact rheometer. Worn surfaces were analyzed using scanning electron microscope (SEM) and electron dispersive spectroscopy (EDS) to study the wear mechanism involved.

2. MATERIALS AND METHODS

2.1 Materials

For disc, AZ91 magnesium alloy, and balls (dia: 10 mm), AISI-52100 stainless steel was used. AZ91 was procured from Exclusive Mg alloy Pvt. Ltd. The approximate chemical composition (weight %) is given as; Ni: 0.001, Cu: 0.08, Zn: 0.84, Fe: 0.02, Al: 9.2, Mn: 0.22, Si: 0.14, and Mg: 89.57. The surfaces of AZ91 magnesium alloy samples were prepared by abrasive grinding using emery papers of different grit sizes (i.e., 180 for rough grinding and 220 to 2000 for fine grinding) and then polished using water suspension of alumina powder as per ASTM E3-95 Standard. Mirror-like finish was obtained by using a special-purpose polishing cloth with diamond paste. Fig. 1 shows the optical image of the polished surface of AZ91.

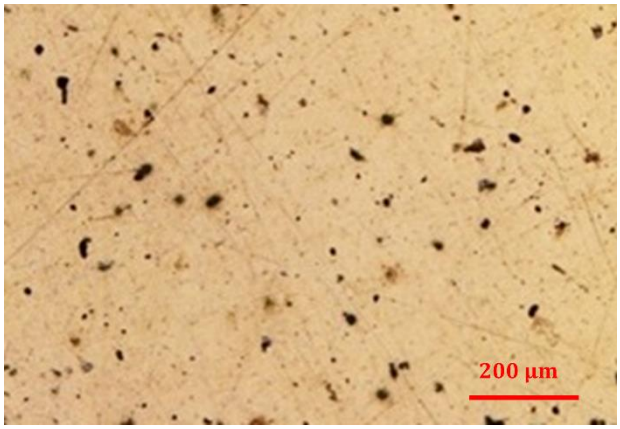

Fig. 1. Optical image of AZ91 disc before the test.

PAO4 used in the study was procured from Aero Biotechniques Ltd. New Delhi. The properties of PAO4 are given in Table 1 as provided by the supplier of PAO4 oil. GNP and h-BN NPs (approximate particle size: 60-100 nm) were purchased from Nanoshel Pvt. Ltd. USA.

Table 1. Typical properties of Poly alpha olefin oil 4.

Sr. No.	Property	Value
1	Kinematic viscosity (cSt) at 100°C	4.1
2	Kinematic viscosity (cSt) @ 40°C	18.50
3	Kinematic viscosity (cSt) @ -40°C	2800
4	Viscosity Index	124
5	Pour Point (°C)	-65
6	Flash Point (°C)	204
7	Specific Gravity at 15.6°C	0.830
8	Density (lb/gal)	6.820

Field emission scanning electron microscope (FESEM) micrographs (Fig. 2a and b) show the morphology of the nanaoparticles. Fig. 2 (a) shows the flaked or 2D layered shape of GNP. Fig. 2 (b) shows the round shape of h-BN NPs, and these are nearly uniform. The layered structure and the weak interaction between the layers of GNP provides easy sliding between these layers resulting in the reduction in friction between two surfaces.

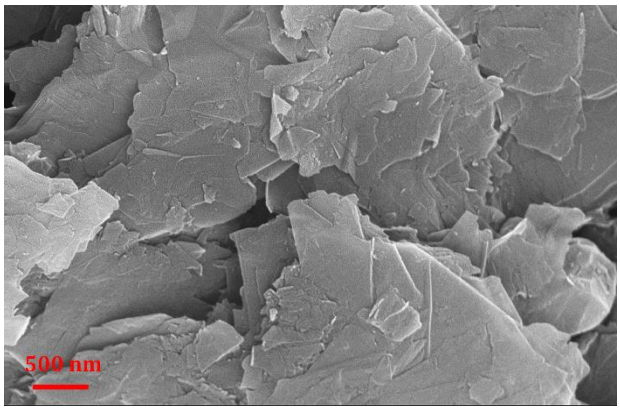

(a)

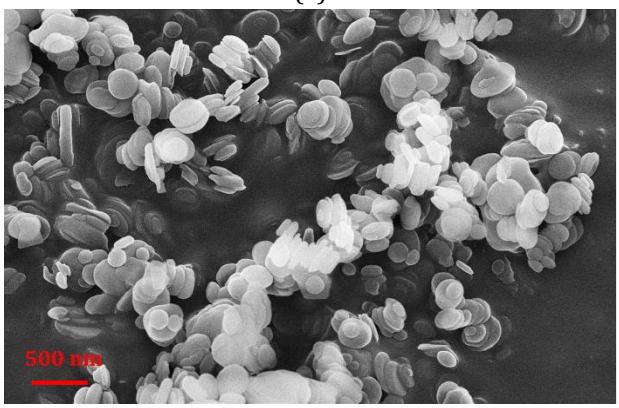

(b)

Fig. 2. FESEM micrographs of the nanoparticles used as nanoadditives: (a) GNP; and (b) h-BN NPs.Fig. 3 (a) and (b) shows the XRD spectrum of h-BN NPs and GNP respectivly.

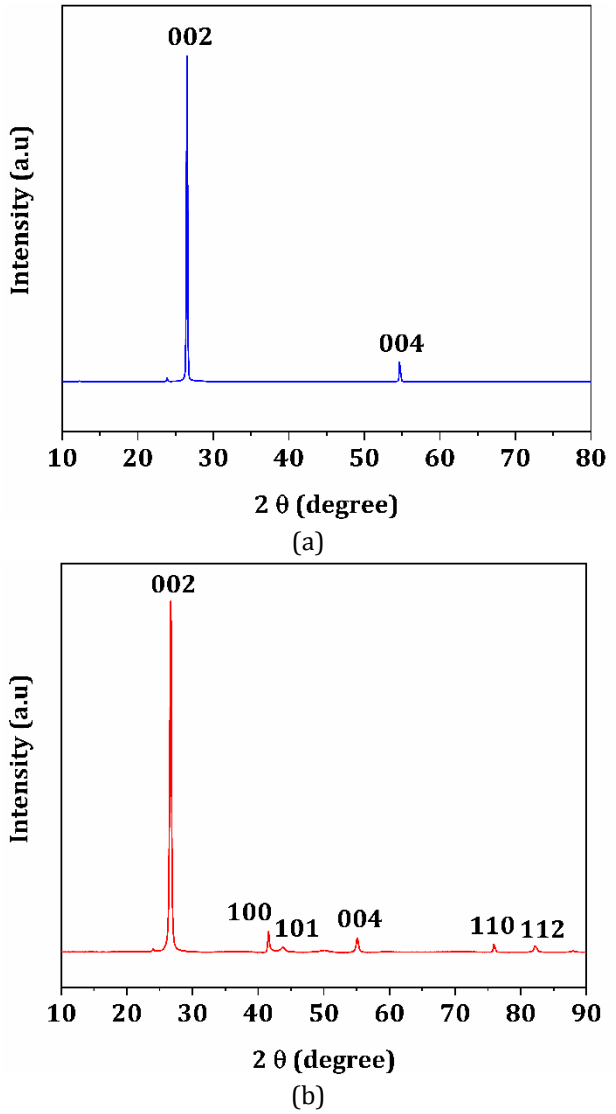

Fig. 3. XRD spectrum of: (a) GNP; and (b) h-BN NPs.

The XRD spectrum of GNP (Fig. 3a) shows the major peak at 2θ=26.5° and a minor peak at 2θ=54.6° corresponding to the miller indeces 002 and 004 respectively. Siburian et al. [32] and Park et. al [33] also reported the similar XRD spectrum for graphite powder.The XRD spectrum of h-BN (Fig. 3b) shows the major peak at 2θ=26.6° corresponding to miller indeces 002. Some minor peaks are also present at 2θ= 41.5°, 43.6 °, 55.1 °, 75.8 ° and 82.12 ° corresponding to the miller indeces 100, 101, 004, 110 and 112. Turkez et. al. [34] and Matovic et. al [35] also reported the similar spectrum of XRD for h-BN nanoparticles.

2.2 Nanolubricants preparation

The h-BN and GNP NPs were dispersed in PAO4 oil to prepare the nanolubricants. The suspensions were prepared by treating the solution ultrasonically using a prob sonicator. Different concentrations (weight %) of GNP and h-BN NPs (i.e., 0.05, 0.1, 0.15 and 0.20) were dispersed in PAO4. To ensure the uniform mixing of the NPs in the oil, each suspension was sonicated for 3 hr 30 min.

2.3 Rheological measurements

The rheological properties of prepared samples were measured using rheometer (Anton Paar, MCR-102) using cone and plate geometry (CP-40) at 0.1 mm gap, as shown in Fig. 4. Controlled shear rate mode (CSR) was used to determine the viscosity and shear stress properties of the prepared nanolubricants following DIN 53019/ISO 3219 Standard. Moreover, rheological experiments were conducted on the base lubricant and NP-based lubricant (i.e., PAO4 & PAO4 with 0.1 % GNP and h-BN) at 25 °C and 40 °C.

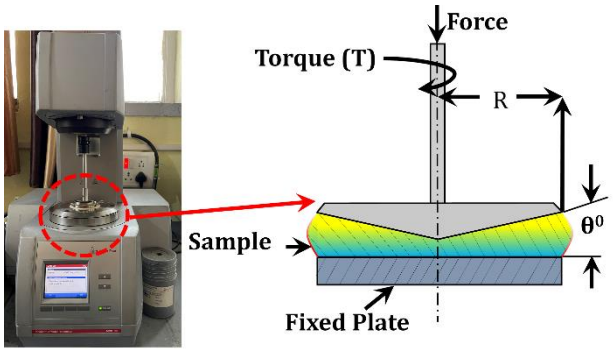

Fig. 4. Photographic and schematic representation of rheometer.

2.4 Tribological testing

A universal tribometer (R. tech Instruments, USA) was used to perform the tribological tests, and the schematic diagram is shown in Fig. 5. A fixed amplitude of 50 μm was used to simulate the fretting tests. Load tests were conducted at; 50 N, 75 N, 100 N, 125 N and 150 N. All tests were performed for a fixed duration of 2.5 hours. Lubricated tests were conducted keeping the samples submerged under 75 ml lubricant. Samples were cleaned using an ultrasonic bath for 30 minutes with ethanol before and after the experiments. After cleaning, samples were dried in an oven for 15 minutes at 50 °C. The wear scar on the ball and disc was measured using an optical microscope to calculate the wear volume. Worn surfaces were analyzed using scanning electron microscopy (SEM) to determine the wear mechanism involved.

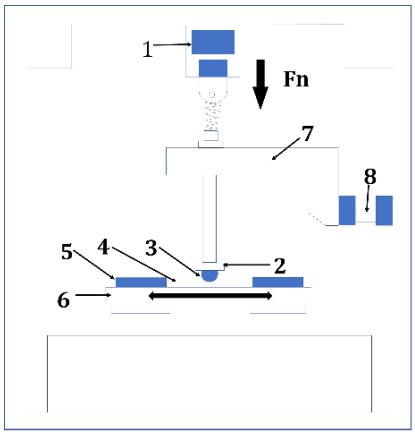

1.Load actuator
2.Ball holder
3.Ball specimen
4.Disc specimen
5.Clamp for disc specimen
6.Reciprocating drive
7.Loading arm
8.Piezoelectric load sensor

Fig. 5. Schematic representation of universal tribometer.

Tests were performed under boundary lubrication as per the given Equation (1) [36]:

$$h_{min} = 7.43R\,(10.85e^{-0.31k})\left(\eta u/E'R\right)^{0.65}\left(L/R^2E^*\right)^{-0.21} \quad (1)$$

where:
u is sliding velocity (m/s),
k is parameter of ellipticity,
R is radius (composite) (m),
η is absolute viscosity (Pa s),
E' is elastic modulus (composite) (Pa),
L is Normal load (N) and
h_{min}= Minimum film thickness

$$\frac{1}{R} = \frac{1}{R_a} + \frac{1}{R_b} \quad (3)$$

$$\lambda = \frac{h_{min}}{\sigma^*} \quad (4)$$

$$\sigma^* = \sqrt{(\sigma_a{}^2 + \sigma_b{}^2)} \quad (5)$$

Where:

R_b *is* radius of the disc (infinite),
R_a is ball's radius,
σ^* is the composite surface roughness,
σ_a is the surface roughness of ball,
σ_b is the surface roughness of disk,
v_a is Poisson's ratio for ball material,
v_b is Poisson's ratio for disk material,
E_b *is* modulus of elasticity for disk material and
E_a *is* modulus of elasticity for ball material.

2.5 Calculation of wear volume

Equation (6) gives the wear volume [37]:

$$V_t = L\left[r^2\sin^{-1}\left(\frac{w}{2r}\right) - \frac{w}{2}\left(r^2 - \frac{w^2}{4}\right)^{1/2}\right] + \frac{\pi}{3}\left[2r^3 - 2r^2\left(r^2 - \frac{w^2}{4}\right)^{1/2} - \frac{w^2}{4}\left(r^2 - \frac{w^2}{4}\right)^{1/2}\right] \quad (6)$$

Where:
W is width of wear scar,
V_t is total wear volume and
r is the radius of the ball.

3. RESULTS AND DISCUSSION

3.1 Shear stress behaviour with respect to shear rate

Rheological properties of nano-lubricants were studied at 25 °C and 40 °C on PAO4 with 0.1 % GNP and h-BN NPs and the shear rate was varied from 0 to 1000 s^{-1}. The results are shown in Fig. 6 (a and b). Shear rate and shear stress for lubricants with and without NPs show a linear relationship, proving that the lubricant remains Newtonian after adding GNP and h-BN NPs. Lower shear stress values were obtained at 40 °C for PAO4 with 0.1 % GNP and 0.1 % h-BN NPs as compared to shear stress values obtained at 25 °C temperature as depicted in Fig. 6 (a and b). Similar behavior is reported by Kumar et al. [38].

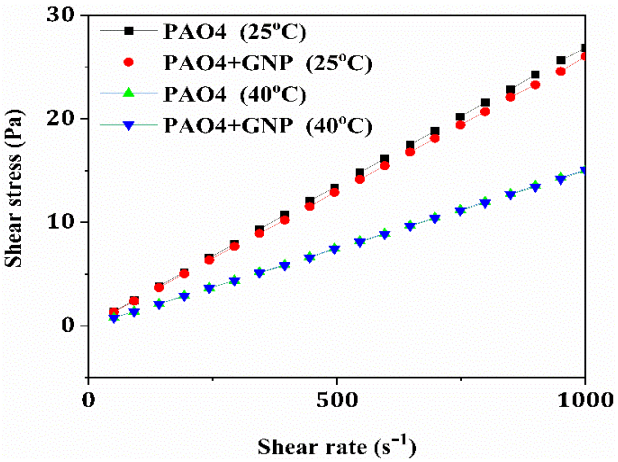

(a)

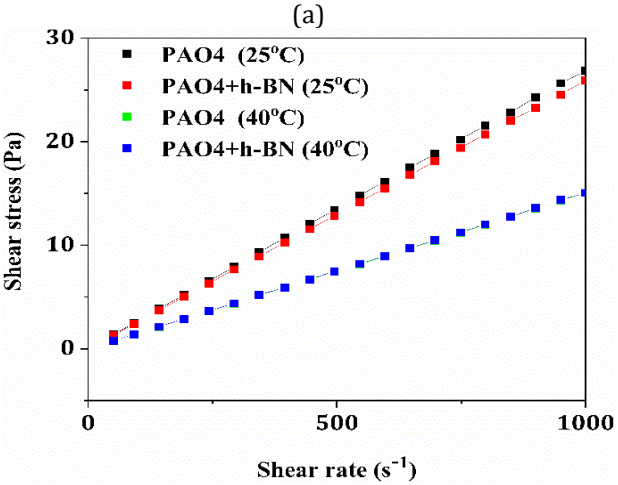

(b)

Fig. 6. Shear stress vs. shear rate of PAO4 with: (a) GNP, (b) h-BN NPs.

3.2 Viscosity behaviour with respect to shear rate

Fig. 7 (a and b), shows the viscosity variation versus shear rate of PAO4 and nano-additives-based PAO4 lubricant. Fig. 7 (a and b) clearly shows that the viscosity nearly remais constant as the shear rate changes. There is no significant effect of nanoparticle addition on viscosity at both temperatures (i.e., 25 °C and 40 °C). This proves that the oil remains Newtonian before and after adding NPs. However, viscosity at 40 °C temperature is lower than that at 25 °C for both the nano-lubricants (i.e., PAO4 with GNP and h-BN NPs). Similar behavior is reported by Kumar et al. [38].

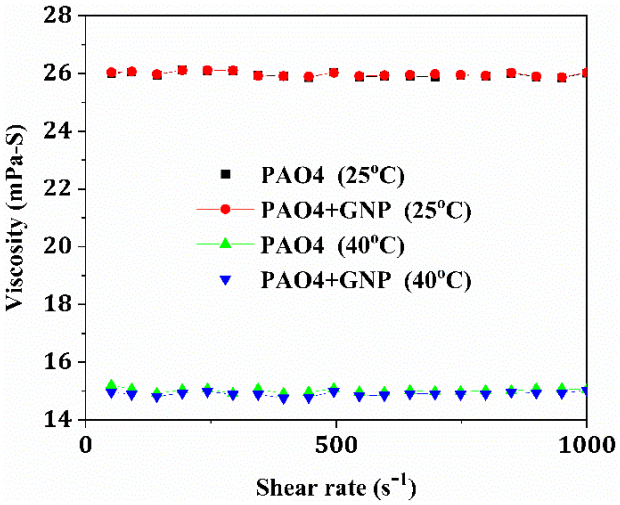

(a)

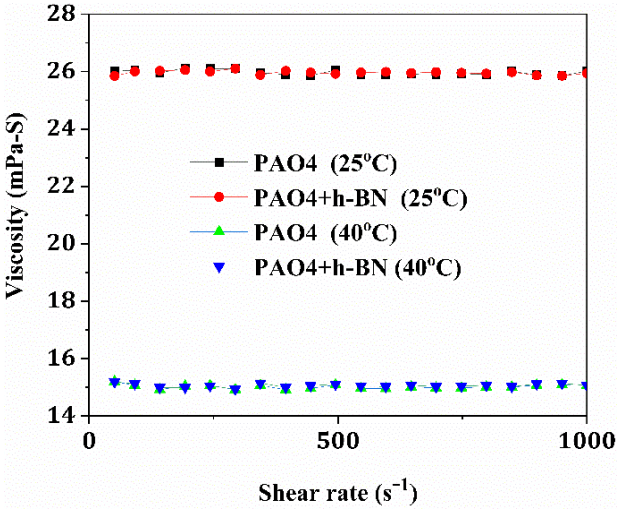

(b)

Fig. 7. Viscosity vs. shear rate for (a) PAO4 base oil and PAO4 with GNP, (b) PAO4 base oil and PAO4 with h-BN NPs.

3.3 Tribological behaviour

(a) Effect of concentration of the nanoparticles on COF

COF decreases as the concentration of NPs in the lubricant increases up to 0.1 weight %, followed by an increase in COF in both cases as shown in Fig. 8. In both cases, the minimum COF was attained at 0.1 weight percent nanoparticle concentration. The NPs' ball-bearing function is thought to cause this, which roll between the mating surfaces and thereby causes a reduction in the COF [15,39,40]. Also, the reduction in COF up to an optimum concentration may be attributed to the filling of asperities by nanoparticles causing a reduction in surface roughness [41]. Beyond 0.1 % concentration, COF increases to a value of 0.070 and 0.085 for GNP and h-BN NPs, respectively. This increasing COF is attributed to the fact that NPs start agglomerating, which fills not only the asperities but also creates some new asperities made of these large agglomerates, which can cause a reduction in the rolling phenomenon of NPs between contact surfaces [42]. Therefore, it is concluded that 0.1 weight % is the optimal nanoparticle concentration for effective reduction in COF for both cases. The lower COF observed in the case of PAO4 + 0.1 % GNP demonstrates the exceptional lubricating property of GNP, which has been attributed to weak interaction and smooth sliding between the layers of GNP [43]. The COF was reduced by 76 % after adding 0.1 % GNP in PAO4. Tolumoye et al. [44] also reported a maximum reduction in COF by about 67 % after adding 2 % GNP. Omrani et. al [45] also reported a maximum improvement in the COF by 10 % after adding 0.7 % of nano graphite in canola oil.

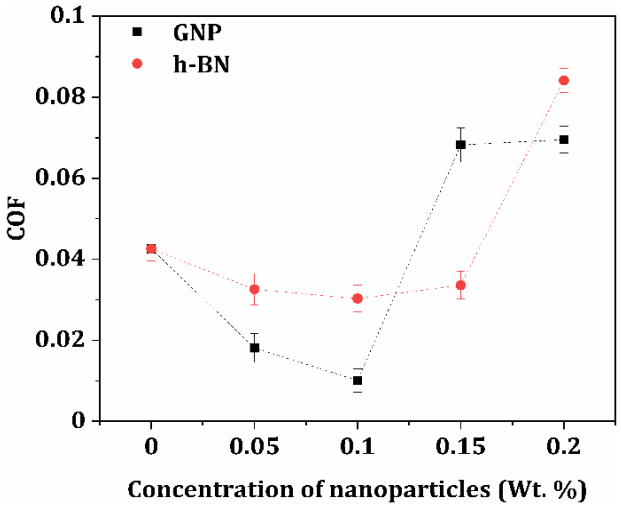

Fig. 8. COF vs. concentration of NPs of graphite and h-BN in PAO4 lubricant.

(b) Effect of concentration of the nanoparticles on wear volume

Fig. 9 shows the variation of wear volume w.r.t the concentration of NPs. The wear volume decreases with increasing the concentration of NPs in the oil up to a concentration of 0.1 weight %. However, beyond 0.1 weight % the increasing concentration of the NPs causes an increase in wear volume in both cases. It is also evident from Fig. 9 that at 0.1 weight %, the wear volume is the least in both cases. This also proves that 0.1 weight % of GNP and h-BN NPs is the optimal concentration for achieving lower COF and wear volume. The mechanism responsible for lower wear, increasing nanoparticle concentration up to optimal concentration, is because of rolling, mending and a protective layer forming between the mating surfaces [28]. As the concentration of NPs increases in the base oil, up to the optimal concentration, they act as nano-bearings between the two surfaces and roll between them, thus preventing direct metal-to-metal contact, which reduces wear. Due to the mending effect, the NPs fill the valleys of the surface (and or micro asperities on the surface), resulting in a smoother surface compared to that without adding NPs [46]. Another reason for wear reduction is the formation of physical deposition film on the sliding surface which prevents direct contact between the metals and consequently reduces wear [47].

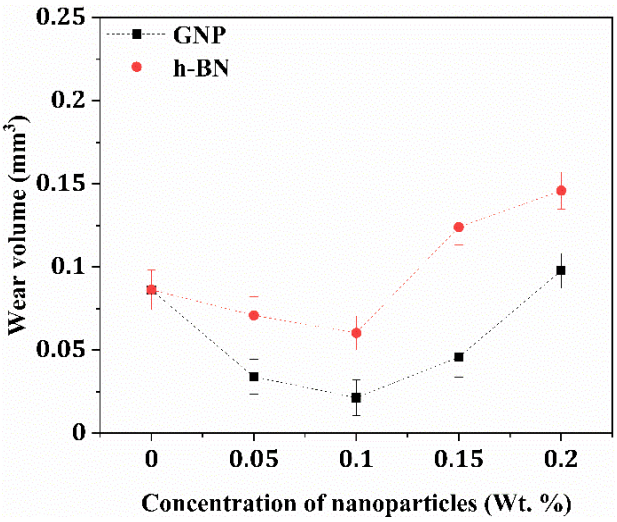

Fig. 9. Wear volume vs. concentration of NPs in PAO4 lubricant.

Beyond the optimal concentration of NPs, wear increases. This may be because the agglomeration of NPs starts after an optimal concentration, which can cause the increment in the size and distortion in the shape of NPs, after which NPs act as a third body between the mating surfaces and the irregular shape of NPs causes abrasion. Another reason is that, beyond the optimal concentration of NPs in the lubricant, the NPs between the contact surfaces may get agglomerated and create other asperities due to the deposition of these large agglomerated particles in the valleys on the surfaces, which may cause the increase in wear [42]. Wear is reduced by the protective boron-rich tribo-film formed by h-BN NPs on the tibo-surface [18]. GNP form a carbon protective film, reducing COF and wear [24]. At all concentrations, wear volumes attained are quite low for GNP. The lower wear volume in case of lubricant with GNP than that with h-BN NPs may be due to the exceptional GNP lubricating property resulting in the smooth sliding between the layers of GNP [43]. The wear volume decreased by 28 % after adding 0.1 % GNP in PAO4 oil. Su et. al. [47] also reported a maximum reduction in the wear volume by 11.44 % after adding GNP in vegitable oil.

(c) Effect of load on COF

All load tests were conducted at 0.1 weight % GNP and h-BN NPs (optimal concentration of nanoparticle). The load was applied in the range of 50 N to 150 N in steps of 25 N. The graph of COF vs. load for PAO4 + 0.1 weight % GNP and PAO4 + 0.1 weight % h-BN NPs is illustrated in Fig. 10.

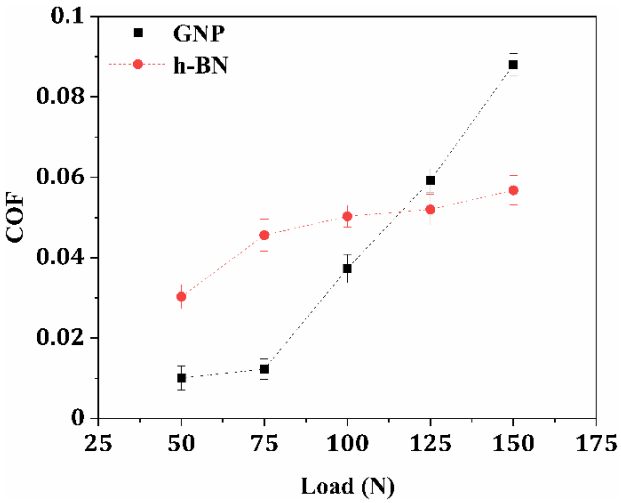

Fig. 10. COF vs. load for PAO4 with 0.1 % GNP and PAO4 with 0.1% h-BN NPs.

It is evident from Fig. 10 that COF increases with increasing the normal load, and this may be due to the increasing contact pressure causing the

formation of more asperity junctions. COF for GNP is lower than h-BN NPs, up to a load of 100N. Beyond this load, higher COF was observed for GNP compared to h-BN NPs. At the highest load of 150 N, the maximum value of COF (0.09) was obtained. Fig. 10 shows that at higher loads, a stable COF was observed for h-BN NPs. So, h-BN NPs perform better at higher loads than GNP. Charoo and Wani [12] and Su et. al, [36] reported similar results.. The lower shear strength of GNP, as compared to that of h-BN NPs, causes the GNP to get distorted and results in increasing contact area between the asperities at higher loads, resulting in a higher COF [18]. Another possible reason for the increase of COF at high loads, in the case of GNP is because of plastic deformation and fracture of NPs. It causes the irregular shape of the NPs, causing the transition of the rolling motion of NPs to a sliding motion, leading to an increase in COF [47]. On the other hand, h-BN NPs can bear a higher load than GNP, providing better frictional performance.

(d) Effect of load on wear volume

Fig. 11 shows the variation of wear volume w.r.t. the normal load for PAO4 + 0.1 weight % GNP and PAO4 + 0.1 weight % h-BN NPs. Fig. 11 clearly shows that wear volume increases with load for both cases; however, for normal loads of 50 N-100 N, the increase in wear volume is negligible for PAO4 + 0.1 weight % h-BN NPs. Under a load of 150N (i.e., the highest load), wear volume is nearly equal for both cases. The wear behavior of AZ91 under PAO4 + 0.1 weight % GNP and PAO4 + 0.1 weight % h-BN NPs is in line with the behavior of COF, as indicated in Fig. 11.

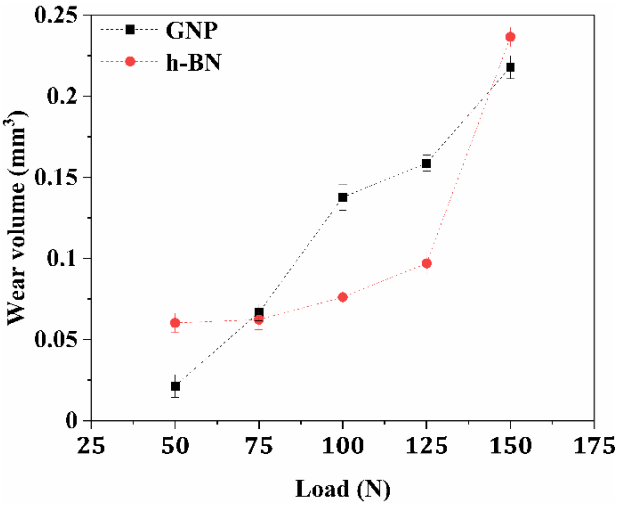

Fig. 11. Wear volume vs. load for PAO4 with 0.1% and PAO4 with 0.1% h-BN NPs.

(e) Worn surface analysis

Worn surfaces were analyzed with an optical microscope, SEM and EDS. The SEM image (Fig. 12b) shows the presence of some delamination and deposition of the material at the worn surface, indicating the dominance of the adhesive wear mechanism under the dry condition, as shown in Fig. 12 (b). The presence of adhesive wear mechanism is due to the direct metalto-metal contact causing the formation of asperity junction under the application of normal load.

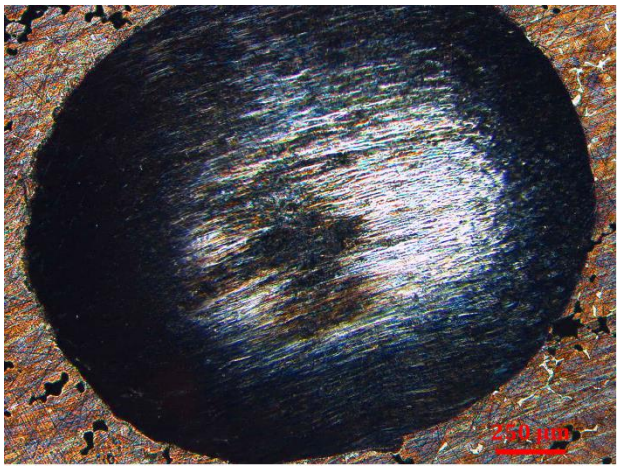

(a)

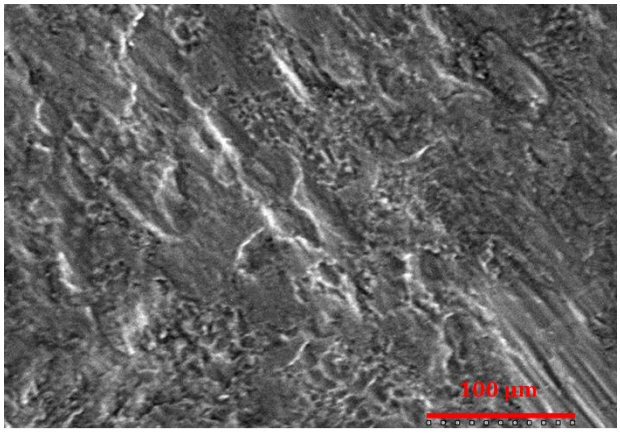

(b)

Fig. 12. Microscopic images of the wear scar generated on the disc under dry condition: (a) Optical microscopic image, (b) SEM image.

Optical and SEM image of worn surface of AZ91 disc under 0.1 weight % GNP based lubricant were obtained after the test, as shown in Fig. 13 (a) and (b). SEM image shows that some layers were removed from the surface (indicated by the rectangular block), which proves the occurrence of delamination. It can also be seen in the EDS analysis in Fig. 13 (c) that carbon is present on the wear surface in a significant amount, which proves the

presence of a protective film of Graphite. The SEM images reveal a smoother worn surface under lubricated conditions than under dry conditions, indicating that the presence of a lubricant layer at the contact interface reduces adhesive wear.

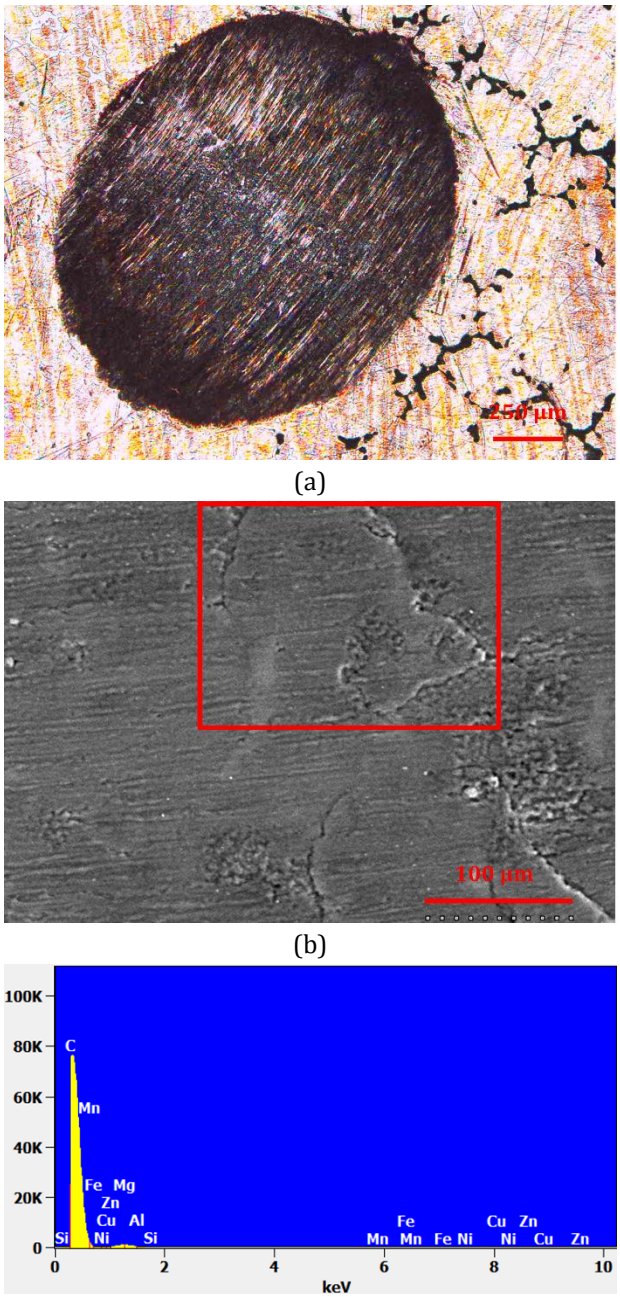

Fig. 13. Worn surface analysis under the lubricated condition (PAO4 with 0.1% GNP) (a) Optical microscopic image of the wear scar generated on the disc, (b) SEM image of the wear scar generated on the disc, (c) EDS elemental graph.

Optical and SEM images of the worn surface of AZ91 disc with 0.1 weight % h-BN NP-based lubricant are shown in Fig. 14 (a) and (b). According to the SEM image, the worn surface is smoother than that obtained under dry fretting conditions, demonstrating how the presence of a lubricant film at the contact interface has reduced adhesive wear. Some wear debris are also present on the surface (indicated by the left-headed arrow) that may be generated by the wear of ball and/or disc material, which the presence of Fe can observe (for ball material) and Al, Mn, and Mg (disc material) in EDS analysis Fig. 14 (c).

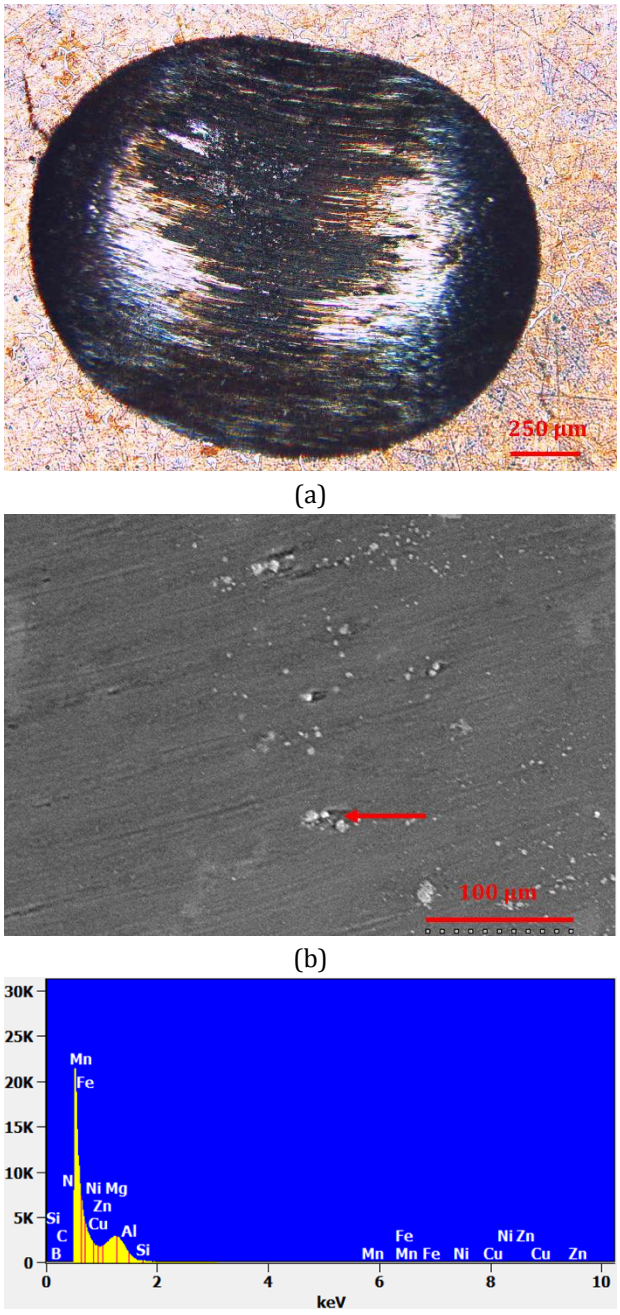

Fig. 14. Worn surface analysis under the lubricated condition (PAO4 with 0.1% h-BN NPs); (a) Optical image of the wear scar generated on the disc, (b) SEM image of the wear scar generated on the disc, (c) EDS elemental graph.

4. CONCLUSION

A study of the influence of nano-lubrication (PAO4 modified with GNP and h-BN NPs) on the tribological response of AZ91 under fretting conditions has been carried out. The major conclusions of this research study are:

- Oil shows the linear relationship between the shear stress and shear rate with and without adding the nanoparticles indicating the Newtonian behavior of the oil after adding the nanoparticles.
- Further, the oil shows constant viscosity with increasing shear rate with and without adding the nanoparticles indicating the Newtonian behavior of the oil after adding the nanoparticles.
- PAO4 modified with 0.1 weight % GNP exhibited the lowest COF (0.0101), while for PAO4 modified with 0.1 weight % h-BN NPs, the COF was found to be 0.0303.
- Wear volume was also minimum for PAO4 with 0.1 weight % GNP, whereas for PAO4 with 0.1 weight % h-BN NPs, wear volume was more.
- COF and wear volume were reduced by 76% and 28%, respectively, using GNP and by 28% and 20%, respectively, using h-BN NPs.
- h-BN NPs resulted in lower COF at higherssss loads; however, the difference between the wear volume at high loads in both cases was negligible.

Hence, GNP gives a better overall performance compared to the base lubricant at lower loads. It can be concluded that GNP can be a very effective lubricant additive in various tribological conditions to improve the lubricating properties of the contacting surface under fretting conditions.

REFERENCES

[1] W. Zhang, J. Xu, *Advanced lightweight materials for Automobiles: A review*, Materials & Design, vol. 221, 2022, doi: doi: 10.1016/j.matdes.2022.110994

[2] A.A. Basheer, *Advances in the smart materials applications in the aerospace industries*, Aircraft Engineering and Aerospace Technology, vol. 92, iss. 7, pp. 1027–1035, 2020, doi: 10.1108/AEAT-02-2020-0040

[3] A. Barhoum, M. García-Betancourt, J. Jeevanandam, E. Hussien, S.A. Mekkawy, M. Mostafa, M. Omran, M.S. Abdalla, M. Bechelany, *Review on natural, incidental, bioinspired, and engineered nanomaterials: history, definitions, classifications, synthesis, properties, market, toxicities, risks, and regulations*, Nanomaterials, vol. 12, iss. 2, 2022, doi: 10.3390/nano12020177

[4] X. Han, A. Alu, H. Liu , Y. Shi, X. Wei, L. Cai, Y. Wei, Biomaterial-assisted biotherapy: A brief review of biomaterials used in drug delivery, vaccine development, gene therapy, and stem cell therapy, Bioactive Materials, vol. 17, pp. 29–48, 2022, doi: 10.1016/j.bioactmat.2022.01.011

[5] I. Ali, O.M.L. Alharbi, Z.A. ALOthman, A. Alwarthan, A.M. Al-Mohaimeed, *Preparation of a carboxymethylcellulose-iron composite for uptake of atorvastatin in water*, International Journal of Biological Macromolecules, vol. 132, pp. 244–253, 2019, doi: 10.1016/j.ijbiomac.2019.03.211

[6] L.H. Hihara, *Advanced materials for corrosion resistant coatings*, Corrosion Reviews, vol. 36, iss. 2, pp. 115–116, 2018, doi: 10.1515/corrrev-2018-0005

[7] B.L. Mordike, T. Ebert, *Magnesium: properties—applications—potential*, Materials Science and Engineering: A, vol. 302, iss. 1, pp. 37–45, 2001, doi: 10.1016/S0921-5093(00)01351-4

[8] D.S. Mehta, S.H. Masood, W.Q. Song, *Investigation of wear properties of magnesium and aluminum alloys for automotive applications*, Journal of Materials Processing Technology, vol. 155, pp. 1526–1531, 2004, doi: 10.1016/j.jmatprotec.2004.04.247

[9] D. Khabale, M.F. Wani, *Tribological Characterization of AZ91 and AE42 Magnesium Alloys in Fretting Contact*, Journal of Tribology, vol. 140, iss. 1, pp. 1-21, 2018, doi: 10.1115/1.4036922

[10] M.F. Wani, *Fretting wear of SiAlON ceramic*, Proceedings of the Institution of Mechanical Engineers, Part J: Journal of Engineering Tribology Institution of Mechanical Engineers, vol. 221, iss. 6, pp. 653–659, 2007, doi: 10.1243/13506501JET233

[11] C. Liang, X. Han, T.F. Su, C. Li, J. An, *Sliding wear map for AZ31 magnesium alloy*, Tribology Transactions, vol. 57, iss. 6, pp. 1077–1085, 2014, doi: 10.1080/10402004.2014.933939

[12] W. Huang, B. Hou, Y. Pang, Z. Zhou, *Fretting wear behavior of AZ91D and AM60B magnesium alloys*, Wear, vol. 260, iss. 11–12, pp. 1173–1178, 2006, doi: 10.1016/j.wear.2005.07.023

[13] V. Saini, J. Bijwe, S. Seth, S.S.V. Ramakumar, *Interfacial interaction of PTFE sub-micron particles in oil with steel surfaces as excellent extreme-pressure additive*, Journal of Molecular Liquids, vol. 325, 2020, doi: 10.1016/j.molliq.2020.115238

[14] A.P.S. Lodhi, D. Kumar, *Natural ingredients based environmental friendly metalworking fluid with superior lubricity*, Colloids and Surfaces A: Physicochemical and Engineering Aspects, vol. 613, 2020, doi: 10.1016/j.colsurfa.2020.126071

[15] C.-G. Lee, Y.-J. Hwang, Y.-M. Choi, J.-K. Lee, C. Choi, J.-M. Oh, *A study on the tribological characteristics of graphite nano lubricants*, International Journal of Precision Engineering and Manufacturing, vol. 10, iss. 1, pp. 85–90, 2009, doi: 10.1007/s12541-009-0013-4

[16] D. Zheng, Y. Wu, Z. Li, Z. Cai, *Tribological properties of WS 2/graphene nanocomposites as lubricating oil additives*, RSC Advances, vol. 7, iss. 23, pp. 14060–14068, 2017, doi: /10.1039/C6RA28028E

[17] P. Kumar, M.F. Wani, *Tribological characterisation of graphene oxide as lubricant additive on hypereutectic Al-25Si/steel tribopair*, Tribology Transactions, vol. 61, iss. 2, pp. 335–346, 2018, doi: 10.1080/10402004.2017.1322735

[18] M.S. Charoo, M.F. Wani, *Tribological properties of h-BN nanoparticles as lubricant additive on cylinder liner and piston ring*, Lubrication Science, vol. 29, iss. 4, pp. 241–254, 2017, doi: 10.1002/ls.1366

[19] M.S. Charoo, M.F. Wani, *Friction and wear properties of nano-Si 3 N 4/nano-SiC composite under nanolubricated conditions*, Journal of Advanced Ceramics, vol. 5, iss. 2, pp. 145–152, 2016, doi: 10.1007/s40145-016-0183-3

[20] V. Saini, J. Bijwe, S. Seth, S.S.V. Ramakumar, *Role of base oils in developing extreme pressure lubricants by exploring nano-PTFE particles*, Tribology International, vol. 143, 2020, doi: 10.1016/j.triboint.2019.106071

[21] I. Ali, A. Basheer, A. Kucherova, N. Memetov, T. Pasko, K. Ovchinnikov, V. Pershin, D. Kuznetsov, E. Galunin, V. Grachev, A. Tkachev, *Advances in carbon nanomaterials as lubricants modifiers*, Journal of Molecular Liquids, vol. 279, pp. 251–266, 2019, doi: doi: 10.1016/j.molliq.2019.01.113

[22] V. Saini, J. Bijwe, S. Seth, S.S.V. Ramakumar, *Potential exploration of nano-talc particles for enhancing the anti-wear and extreme pressure performance of oil*, Tribology International, vol. 151, 2020, doi: 10.1016/j.triboint.2020.106452

[23] P.D. Srivyas, M.S. Charoo, *Tribological behaviour of nano additive based PAO lubricant for eutectic Al-Si alloy-chromium plated chrome steel tribopair*, Materials Today: Proceedings, vol. 151, pp. 1-6, 2020, doi: 10.1016/j.matpr.2020.04.784

[24] P.D. Srivyas, M.S. Charoo, *Nano lubrication behaviour of Graphite, h-BN and Graphene Nano Platelets for reducing friction and wear*, Materials Today: Proceedings, vol. 44, pp. 7-11, 2020, doi: 10.1016/j.matpr.2020.04.785

[25] T. Zolper, Z. Li, C. Chen, M. Jungk, T. Marks, Y.W. Chung, Q. Wang, *Lubrication properties of polyalphaolefin and polysiloxane lubricants: molecular structure–tribology relationships*, Tribology Letters, vol. 48, iss. 3, pp. 355–365, 2012, doi: 10.1007/s11249-012-0030-9

[26] S.D. Fayaz, M.F. Wani, *Evaluating Scuffing Failure in Dry Sliding Conditions of Monolayer Chromium Piston Ring/Bulk Grey Cast Iron Liner Interface*, Tribology Online, vol. 15, iss. 1, pp. 9–17, 2020, doi: /10.2474/trol.15.9

[27] D. Syed, M.F. Wani, Tribological behavior of chrome-deposited SAE9254 grade steel top compression piston ring under lubrication starvation and mild extreme pressure lubrication, International Journal of Engine Research, vol. 22, iss. 4, 2019, doi: 10.1177/1468087419890995

[28] P. Kumar, M.F. Wani, *Effect of temperature on the friction and wear properties of graphene nano-platelets as lubricant additive on Al-25Si alloy*, Materials Research Express, vol. 6, iss. 4, 2019, doi: 10.1088/2053-1591/aafb46

[29] A. Kontou, R.I. Taylor, H.A. Spikes, *Effects of dispersant and ZDDP additives on fretting wear*, Tribology Letters, vol. 69, iss. 1, 2021. doi: 10.1007/s11249-020-01379-6

[30] I. Mahdi, R. Garg, A. Srivastav, *ZDDP-An inevitable lubricant additive for engine oils*, International Journal of Engineering Inventions, vol. 1, no. 1, pp. 47–48, 2012.

[31] H. Spikes, *Low-and zero-sulphated ash, phosphorus and sulphur anti-wear additives for engine oils*, Lubrication Science, vol. 20, iss. 2, pp. 103–136, 2008, doi: 10.1002/ls.57

[32] R. Siburian, C. Simanjuntak, M. Supeno, S. Lumbanraja, H. Sihotang, *New route to synthesize of graphene nano sheets*, Oriental journal of chemistry, vol. 34, no. 1, pp. 182-187, 2018.

[33] W.K. Park, Y. Yoon, Y.H. Song, S.Y. Choi, S. Kim, Y. Do, J. Lee, H. Park, D.H. Yoon, W.S. Yang, *High-efficiency exfoliation of large-area mono-layer graphene oxide with controlled dimension*, Scientific reports, vol. 7, iss. 1, 2017, doi: 10.1038/s41598-017-16649-y

[34] H. Türkez, M.E. Arslan, E. Sönmez, M. Açikyildiz, A. Tatar, F. Geyikoğlu, *Synthesis, characterization and cytotoxicity of boron nitride nanoparticles: Emphasis on toxicogenomics*, Cytotechnology, vol. 71, pp. 351–361, 2019, doi: 10.1007/s10616-019-00292-8

[35] B. Matović, J. Luković, M. Nikolic, B. Babic, N. Stankovic, B. Jokić, B. Jelenković, *Synthesis and characterization of nanocrystaline hexagonal boron nitride powders: XRD and luminescence properties*, Ceramics International, vol. 42, iss. 15, pp. 16655–16658, 2016. doi: 10.1016/j.ceramint.2016.07.096

[36] A. Raina, A. Anand, *Tribological investigation of diamond nanoparticles for steel/steel contacts in boundary lubrication regime*, Applied Nanoscience, vol. 7, iss. 7, pp. 371–388, 2017, doi: 10.1007/s13204-017-0590-y

[37] S. Sharma, S. Sangal, K. Mondal, *On the optical microscopic method for the determination of ball-on-flat surface linearly reciprocating sliding wear volume*, Wear, vol. 300, iss. 1–2, pp. 82–89, 2013, doi: 10.1016/j.wear.2013.01.107

[38] S. Kumar, M. F. Wani, R. Sehgal, S. Mushtaq, *Friction and Wear Properties of Si3N4/TiC Ceramic Composite under Nano Lubrication*, in Journal of Physics: Conference Series, vol. 1240, iss. 1, 2019, doi: 10.1088/1742-6596/1240/1/012134

[39] M.K.A. Ali, H. Xianjun, L. Mai, C. Qingping, R.F. Turkson, C. Bicheng, Improving the tribological characteristics of piston ring assembly in automotive engines using Al2O3 and TiO2 nanomaterials as nano-lubricant additives, Tribology International, vol. 103, pp. 540–554, 2016, doi: 10.1016/j.triboint.2016.08.011

[40] M.K.A. Ali, H. Xianjun, Exploring the lubrication mechanism of CeO2 nanoparticles dispersed in engine oil by bis (2-ethylhexyl) phosphate as a novel antiwear additive, Tribology International, vol. 165, 2022, doi: 10.1016/j.triboint.2021.107321

[41] M.K.A. Ali, H. Xianjun, M.A.A. Abdelkareem, M. Gulzar, A.H. Elsheikh, *Novel approach of the graphene nanolubricant for energy saving via anti-friction/wear in automobile engines*, Tribology International, vol. 124, pp. 209–229, 2018. doi: 10.1016/j.triboint.2018.04.004

[42] Q. Wan, Y. Jin, P. Sun, Y. Ding, *Tribological behaviour of a lubricant oil containing boron nitride nanoparticles*, Procedia Engineering, vol. 102, pp. 1038–1045, 2015, doi: 10.1016/j.proeng.2015.01.226

[43] J. Li, T. Gao, J. Luo, *Superlubricity of graphite induced by multiple transferred graphene nanoflakes*, Advanced Science, vol. 5, iss. 3, 2018, doi: doi.org/10.1002/advs.201700616

[44] T.J. Tuaweri, T J. Ajoko, K. Kotingo, *Effect of Graphite Nanoparticles on the Friction Characteristics of Palm Oil*, International Journal of Engineering and Information Systems (IJEAIS), vol. 3, iss. 2, 2018, https://philpapers.org/rec/TUAEOG

[45] E. Omrani, P.L. Menezes, P.K. Rohatgi, *Effect of Micro- and Nano-Sized Carbonous Solid Lubricants as Oil Additives in Nanofluid on Tribological Properties*, Lubricants, vol. 7, iss. 3. 2019, doi: 10.3390/lubricants7030025

[46] G. Liu, X. Li, B. Qin, D. Xing, Y. Guo, R. Fan, *Investigation of the mending effect and mechanism of copper nano-particles on a tribologically stressed surface*, Tribology Letters., vol. 17, iss. 4, pp. 961–966, 2004, doi: 10.1007/s11249-004-8109-6

[47] Y. Su, L. Gong, D. Chen, *An investigation on tribological properties and lubrication mechanism of graphite nanoparticles as vegetable based oil additive*, Journal of Nanomaterials, vol. 2015, 2015, doi: 10.1155/2015/276753